Chen-Hao Luo, Rui Wang, Roberto F. Weinberg, and Zengqian Hou, 2021, Isotopic spatial-temporal evolution of magmatic rocks in the Gangdese belt: Implications for the origin of Miocene post-collisional giant porphyry deposits in southern Tibet: GSA Bulletin, https://doi.org/10.1130/B36018.1.

Supplemental Material

Figure S1. Nd-Hf isotopically spatial distribution (isotopic fingerprint) of representative data of the Jurassic, Cretaceous, Paleocene-Eocene and Miocene magmatic rocks in the Gangdese belt, southern Tibet (use the highest isotopic value per 0.5 longitude, and the average isotopic values of per 0.5 longitude as representative data, Nd isotopic data was analyzed from the whole-rocks samples, and the Hf isotopic data was analyzed from the zircon samples). A-D. εNd(t = 15 Ma) versus longitude. E-H. zircon εHf(t = 15 Ma) versus longitude.

Figure S2. Magma mixing modeling for generation of Miocene high-Sr/Y granitoid magmas in the Gangdese belt, southern Tibet, using the trachytic melt represented by Chazi dyke sample ZFC004 from Guo et al. (2015) and Gangdese belt Jurassic (A) and Cretaceous (B) magmatic rock samples. Nd isotopic data was analyzed from the whole-rocks samples, all samples used are the ones with the maximum $\varepsilon Nd_{(t = 15\ Ma)}$ per 0.5 longitude (Table S4). The calculations use $Nd_M = Nd_A f_A + Nd_B(1 - f_A)$, $\varepsilon Nd_M = \varepsilon Nd_A f_A \frac{Nd_A}{Nd_M} + \varepsilon Nd_B\ （1 - f_A）\ \frac{Nd_B}{Nd_M}$. Nd_A, Nd_B and Nd_M are the Nd content of the two mixed magmas and mixture respectively, εNd_A, εNd_B and εNd_M are the $\varepsilon Nd_{(t)}$ of the two mixed magmas and mixture respectively, f is the involved proportion. The Nd content of the lower crust used is 25 ppm, which is the average value of global lower crust, from Gao et al. (1998).

Table S1. Major and trace element compositions of the subduction and collision-related magmatic rocks in the Gangdese belt, southern Tibet

Table S2. Sr-Nd isotope data of the the subduction and collision-related magmatic rocks in the Gangdese belt, southern Tibet

Table S3. Zircon Hf isotope data of the subduction and collision-related magmatic rocks in the Gangdese belt, southern Tibet

Table S4. Sr-Nd isotope data used for the magma mixing modeling

Table S5. Lu-Hf isotope data of the inherited zircons in Miocene magmatic rocks in the Gangdese belt, southern Tibet

REFERENCES CITED

Chen, L., Qin K.Z., Li G.M., Li, J.X., Xiao, B., Zhao, J.X., Xin, Fan., 2015, Zircon U–Pb ages, geochemistry, and Sr–Nd–Pb–Hf isotopes of the Nuri intrusive rocks in the Gangdese area, southern Tibet: Constraints on timing, petrogenesis, and tectonic transformation: Lithos, v. 212-215, p. 379–396, https://doi.org/10.1016/j.lithos.2014.11.014.

Chen, R., Liu, Y.L., Guo, L.S., Wang, Z.H., Liu, H.F., Xu, K.F., and Zhang, J.S., 2014, Geochronology and Geochemistry of the Tinggong Porphyry Copper Ore Deposit, Tibet: Acta Geologica Sinica-english Edition, v. 88, p. 780–800, https://doi.org/10.1111/1755-6724.12238.

Chu, M.F., Chung, S.L., Oreilly, S.Y., Pearson, N.J., Wu, F.Y., Li, X.H., Liu, D.Y., Ji, J.Q., Chu, C.H., and Lee, H.Y., 2011, India's hidden inputs to Tibetan orogeny revealed by Hf isotopes of Transhimalayan zircons and host rocks: Earth and Planetary Science Letters, v. 307, p. 479–486, https://doi.org/10.1016/j.epsl.2011.05.020.

Chu, M.F., Chung, S.L., O'Reilly, S.Y., Pearson, N.J., and Lee, H.Y., 2011, India's hidden inputs to tibetan orogeny revealed by hf isotopes of transhimalayan zircons and host rocks: Earth and Planetary Science Letters, v. 307, p. 479–486, https://doi.org/10.1016/j.epsl.2011.05.020.

Chung, S.L., Chu, M.F., Ji, J.Q., O'Reilly, S.Y., Pearson, N.J., Liu, D.Y., Lee, T.Y., and Lo, C.H., 2009, The nature and timing of crustal thickening in Southern Tibet: Geochemical and zircon Hf isotopic constraints from post-collisional adakites: Tectonophysics, v. 477, p. 36–48, https://doi.org/10.1016/j.tecto.2009.08.008.

Dong, X., and Zhang, Z.M., 2013, Genesis and tectonic significance of the Early Jurassic magmatic rocks from the southern Lhasa terrane [in Chinese]: Yanshi Xuebao, v. 29, p. 1933–1948.

Gao, Y.F., Hou, Z.Q., Kamber, B.S., Wei, R.H., Meng, X.G., and Zhao, R.S., 2007, Adakite-like porphyries from the southern Tibetan continental collision zones: evidence for slab melt metasomatism: Contributions to Mineralogy and Petrology, v. 153, p. 105–120, https://doi.org/10.1007/s00410-006-0137-9.

Gao, Y.F., Yang, Z.S., Santosh, M., Hou, Z.Q., Wei, R.H., and Tian, S.H., 2010, Adakitic rocks from slab melt-modified mantle sources in the continental collision zone of southern Tibet: Lithos, v. 119, p. 651–663, https://doi.org/10.1016/j.lithos.2010.08.018.

Guo, L.S., Liu, Y.L., Liu, S., Cawood, P.A., Wang, Z.H., and Liu, H.F., 2013, Petrogenesis of early to middle jurassic granitoid rocks from the gangdese belt, southern tibet: implications for early history of the neo-tethys: Lithos, v. 179, p. 320–333, https://doi.org/10.1016/j.lithos.2013.06.011.

Guo, L., Z, H.F., Harris, N., Luo, B.J., Zhang, W., Xu, W.C., 2019, Tectonic erosion and crustal relamination during the India-Asian continental collision: Insights from Eocene magmatism in the southeastern Gangdese belt: Lithos, v. 346–347, https://doi.org/10.1016/j.lithos.2019.105161.

Guo, Z.F., Wilson, M., Zhang, M.L., Cheng, Z.H., and Zhang, L.H., 2015, Post-collisional ultrapotassic mafic magmatism in south tibet: products of partial melting of pyroxenite in the mantle wedge induced by roll-back and delamination of the subducted indian continental lithosphere slab: Journal of Petrology, v. 56, p. 1365–1406, https://doi.org/10.1093/petrology/egv040.

Hou, Z.Q., Gao, Y.F., Qu, X.M., Rui, Z.Y., and Mo, X.X., 2004, Origin of adakitic intrusives generated during mid-Miocene east–west extension in southern Tibet: Earth and Planetary Science Letters, v. 220, p. 139–155, https://doi.org/10.1016/S0012-821X(04)00007-X.

Hou, Z.Q., Yang, Z.M., Lu, Y.J., Kemp, A., Zheng, Y.C., Li, Q.Y., Tang, J.X., Yang, Z.S., and Duan, L.F., 2015, A genetic linkage between subduction- and collision-related porphyry Cu deposits in continental collision zones: Geology, v. 43, p. 247–250, https://doi.org/10.1130/G36362.1.

Hou, Z.Q., Zheng, Y.C., Yang, Z.M., Rui, Z.Y., Zhao, Z.D., Jiang, S.H., Qu, X.M., and Sun, Q.Z., 2013, Contribution of mantle components within juvenile lower-crust to collisional zone porphyry Cu systems in Tibet: Mineralium Deposita, v. 48, p. 173–192, https://doi.org/10.1007/s00126-012-0415-6.

Hu, Y.B., Liu, J.Q., Hu, J.R., Ding, X., Sun, W.D., Liu, Y., and Ling, M.X., 2015, Geochemical studies on ore-bearing rocks in Bangpu porphyry Mo (Cu)deposit,Tibet:Implications on the magma source and metallogenic mechanism [in Chinese]: Yanshi Xuebao, v. 31, p. 2038–2052.

Hu, Y.B., Liu, J.Q., Ling, M.X., Liu, Y., Ding, X., Liu, D.Y., and Sun, W.D., 2017, Constraints on the origin of adakites and porphyry Cu-Mo mineralization in Chongjiang, Southern Gangdese, the Tibetan Plateau: Lithos, v. 292–293, p. 424–436, https://doi.org/10.1016/j.lithos.2017.09.012.

Huang, F., Li, M.J., Xu, J.F., Zeng, Y.C., Chen, J.L., Wang, B.D., Yu, H.X., Chen, L., Zhao, P.P., and Zhang, Z., 2019, Geodynamic transition from subduction to extension: evidence from the geochronology and geochemistry of granitoids in the Sangsang area, southern Lhasa Terrane, Tibet: International Journal of Earth Sciences, v. 108, p. 1663–1681, https://doi.org/10.1007/s00531-019-01729-3.

Huang, Y., Ding, J., Li, G.M., Dai, J., Yan, G.Q., Wang, G., and Liu, X.F., 2015, U-Pb Dating, Hf Isotopic Characteristics of Zircons from Intrusions in the Zhuluo Porphyry Cu-Mo-Au Deposit and Its Mineralization Significance [in Chinese]: Acta Geologica Sinica, v. 89, p. 99–108.

Huang, Y., Li, G.M., Ding, J., Dai, J., Yan, G.Q., Dong, S.L., and Huang, H.X., 2017, Origin of the Newly Discovered Zhunuo Porphyry Cu-Mo-Au Deposit in the Western Part of the Gangdese Porphyry Copper Belt in the Southern Tibetan Plateau, SW China: Acta Geologica Sinica-english Edition, v. 91, p. 109–134, https://doi.org/10.1111/1755-6724.13066.

Huang, Y., Zhao, Z.D., Zhang, F.Q., Zhu, D.C., Dong, G.C., Zhou, S., and Mo, X.X., 2010, Geochemistry and implication of the Gangdese batholiths fom Renbu and Lhasa areas in southern Gangdese, Tibet [in Chinese]: Yanshi Xuebao, v. 26, p. 3131–3142.

Ji, W.Q., Wu, F.Y., Chung, S.L., Li, J.X., and Liu, C.Z., 2009, Zircon U-Pb geochronology and Hf isotopic constraints on petrogenesis of the Gangdese batholith, southern Tibet: Chemical Geology, v. 262, p. 229–245, https://doi.org/10.1016/j.chemgeo.2009.01.020.

Ji, W.Q., Wu, F.Y., Chung, S.L., and Liu, C.Z., 2014, The Gangdese magmatic constraints on a latest Cretaceous lithospheric delamination of the Lhasa terrane, southern Tibet: Lithos, v. 210-211, p. 168–180, https://doi.org/10.1016/j.lithos.2014.10.001.

Ji, W.Q., Wu, F.Y., Liu, C.Z., and Chung, S.L., 2012, Early Eocene crustal thickening in southern Tibet: New age and geochemical constraints from the Gangdese batholith: Journal of Asian Earth Sciences, v. 53, p. 82–95, https://doi.org/10.1016/j.jseaes.2011.08.020.

Ji, W.Q., Wu, F.Y., Liu, C.Z., and Zhang, H., 2017, Zircon U-Pb geochronology and Hf isotopes of granitic rocks and river sands in the nyingchi region, Tibet: constraints on evolution of the deep crust beneath the southeast lhasa terrane: Journal of Asian Earth Sciences, v. 145, p. 613–625, https://doi.org/10.1016/j.jseaes.2017.07.006.

Jiang, Z.Q., Wang, Q., Li, Z.X., Wyman, D.A., Tang, G.J., Jia, X.H., and Yang, Y.H., 2012, Late Cretaceous (ca. 90 Ma) adakitic intrusive rocks in the Kelu area, Gangdese Belt (southern Tibet): Slab melting and implications for Cu–Au mineralization: Journal of Asian Earth Sciences, v. 53, p. 67–81, https://doi.org/10.1016/j.jseaes.2012.02.010.

Jiang, Z.Q., Wang, Q., Wyman, D.A., Li, Z., Yang, J., Shi, X.B., Ma, L., Tang, G.J., Gou, G.L., Jia, X.H., and Guo, H.F., 2014, Transition from oceanic to continental lithosphere subduction in southern Tibet: Evidence from the Late Cretaceous–Early Oligocene (~91–30 Ma) intrusive rocks in the Chanang-Zedong area, southern Gangdese: Lithos, v. 196–197, p. 213–231, https://doi.org/10.1016/j.lithos.2014.03.001.

Kang, Z.Q., Xu, J.F., Wilde, S.A., Feng, Z.H., Chen, J.L., Wang, B.D., Fu, W.C., and Pan, H.B., 2014, Geochronology and geochemistry of the Sangri Group Volcanic Rocks, Southern Lhasa Terrane: Implications for the early subduction history of the Neo-Tethys and Gangdese Magmatic Arc: Lithos, v. 200-201, p. 157–168, https://doi.org/10.1016/j.lithos.2014.04.019.

Lang, X.H., Wang, X.H., Tang, J.X., Deng, Y.L., Cui, Z.W., Yin, Q., and Xie, F.W., 2018, Composition and age of Jurassic diabase dikes in the Xiongcun porphyry copper–gold district, southern margin of the Lhasa terrane, Tibet, China: Petrogenesis and tectonic setting: Geological Journal, v. 53, p. 1973–1993, https://doi.org/10.1002/gj.3028.

Li, J.X., Qin, K.Z., Li, G.M., Xiao, B., Chen, L., and Zhao, J.X., 2011, Post-collisional ore-bearing adakitic porphyries from Gangdese porphyry copper belt, southern Tibet: Melting of thickened juvenile arc lower crust: Lithos, v. 126, p. 265–277, https://doi.org/10.1016/j.lithos.2011.07.018.

Liu, Z.C., Ding, L., Zhang, L.Y., Wang, C., Qiu, Z.L., Wang, J.G., Shen, X.L., and Deng, X.Q., 2018, Sequence and petrogenesis of the Jurassic volcanic rocks (Yeba Formation) in the Gangdese arc, southern Tibet: Implications for the Neo-Tethyan subduction: Lithos, https://doi.org/10.1016/j.lithos.2018.04.026.

Luo, M.C., Wang, L.Q., Leng, Q.F., and Chen, W., 2011, Zircon Hf isotope and Cet/Ce ratio of the monzogranite porphyry and biotite monzonitic granite in Bangpu Mo(Cu) deposit, Tibet [in Chinese]: Mineral Deposits, v. 30, p. 266–277.

Ma, L., Wang, Q., Wyman, D.A., Jiang, Z.Q., Wu, F.Y., Li, X.H., Yang, J.H., Gou, G.N., and Guo, H.F., 2015, Late Cretaceous back-arc extension and arc system evolution in the Gangdese area, southern Tibet: Geochronological, petrological, and Sr-Nd-Hf-O isotopic evidence from Dagze diabases: Journal of Geophysical Research, v. 120, p. 6159–6181, https://doi.org/10.1002/2015JB011966.

Ma, L., Wang, Q., Wyman, D.A., Jiang, Z.Q., Yang, J.H., Li, Q.L., Guo, G.N., and Guo, H.F., 2013a, Late Cretaceous crustal growth in the Gangdese area, southern Tibet: Petrological and Sr–Nd–Hf–O isotopic evidence from Zhengga diorite–gabbro: Chemical Geology, v. •••, p. 54–70, https://doi.org/10.1016/j.chemgeo.2013.04.005.

Ma, L., Wang, Q., Wyman, D.A., Li, Z.X., Jiang, Z.Q., Yang, J.H., Gou, G.N., and Guo, H.F., 2013b, Late Cretaceous (100–89 Ma) magnesian charnockites with adakitic affinities in the Milin area, eastern Gangdese: Partial melting of subducted oceanic crust and implications

for crustal growth in southern Tibet: Lithos, v. 175–176, p. 315–332, https://doi.org/10.1016/j.lithos.2013.04.006.
Mo, X.X., Dong, G.C., Zhao, Z.D., Zhu, D.C., Zhou, S., and Niu, Y.L., 2008, Mantle input to the crust in Southern Gangdese, Tibet, during the Cenozoic: Zircon Hf isotopic evidence: Journal of Earth Science, v. 20, p. 241–249, https://doi.org/10.1007/s12583-009-0023-2.
Qu, X.M., Xin, H.B., and Xu, W.Y., 2007, Petrogenesis of the Ore- Hosting Volcanic Rocks and Their Contribution to Mineralization in Xiongcun Superlarge Cu- Au Deposit, Tibet [in Chinese]: Acta Geologica Sinica, v. 81, p. 964–971.
Sun, X., Zheng, Y.Y., Li, M., Ouyang, H., Liu, Q.Q., Jing, X.K., Sun, G.P., and Song, Q.J., 2017, Genesis of Luobuzhen Pb–Zn veins: Implications for porphyry Cu systems and exploration targeting at Luobuzhen-Dongshibu in western Gangdese belt, southern Tibet: Ore Geology Reviews, v. 82, p. 252–267, https://doi.org/10.1016/j.oregeorev.2016.11.016.
Tang, Y.W., Chen, L., Zhao, Z.F., and Zheng, Y.F., 2019, Geochemical evidence for the production of granitoids through reworking of the juvenile mafic arc crust in the Gangdese orogen, southern Tibet: Geological Society of America Bulletin, v. 132, no. 7–8, p. 1347–1364, https://doi.org/10.1130/B35304.1.
Wang, B.D., Xu, J.F., Chen, J.L., Zhang, X.G., Wang, L.Q., and Xia, B.B., 2010, Petrogenesis and geochronology of the ore-bearing porphyritic rocks in Tangbula porphyry molybdenum-copper deposit in the eastern segment of the Gangdese metallogenic belt [in Chinese]: Yanshi Xuebao, v. 26, p. 1820–1832.
Wang, C., Ding, L., Zhang, L.Y., Ding, X.L., and Yue, Y.H., 2018, Early Jurassic high-Mg andesites in the Quxu area, southern Lhasa terrane: Implications for magma evolution related to a slab rollback of the Neo-Tethyan Ocean: Geological Journal, v. 54, p. 2508–2524, https://doi.org/10.1002/gj.3309.
Wang, R., Richards, J.P., Hou, Z.Q., An, F., and Creaser, R.A., 2015a, Zircon U–Pb age and Sr–Nd–Hf–O isotope geochemistry of the Paleocene–Eocene igneous rocks in western Gangdese: Evidence for the timing of Neo-Tethyan slab breakoff: Lithos, v. 224–225, p. 179–194, https://doi.org/10.1016/j.lithos.2015.03.003.
Wang, R., Richards, J.P., Zhou, L.M., Hou, Z.Q., Stern, R.A., Creaser, R.A., and Zhu, J.J., 2015b, The role of Indian and Tibetan lithosphere in spatial distribution of Cenozoic magmatism and porphyry Cu–Mo deposits in the Gangdese belt, southern Tibet: Earth-Science Reviews, v. 150, p. 68–94, https://doi.org/10.1016/j.earscirev.2015.07.003.
Wang, R., Richards, J.P., Hou, Z.Q., and Yang, Z.M., 2014, Extent of underthrusting of the Indian plate beneath Tibet controlled the distribution of Miocene porphyry Cu-Mo ± Au deposits: Mineralium Deposita, v. 49, p. 165–173, https://doi.org/10.1007/s00126-013-0507-y.
Wang, R., Tafti, R., Hou, Z.Q., Shen, Z.C., Guo, N., Evans, N.J., Jeon, H., Li, Q.Y., and Li, W.K., 2017, Across-arc geochemical variation in the jurassic magmatic zone, southern tibet: implication for continental arc-related porphyry cuau mineralization: Chemical Geology, v. 451, p. 116–134, https://doi.org/10.1016/j.chemgeo.2017.01.010.
Wang, R.Q., Qiu, J.S., Yu, S.B., and Zhao, J.L., 2017, Crust-mantle interaction during early Jurassic subduction of Neo-tethyan oceanic slab: evidence from the Dongga gabbro-granite complex in the southern Lhasa subterrane, Tibet: Lithos, v. 292-293, p. 262–277, https://doi.org/10.1016/j.lithos.2017.09.018.

Wei, Y.Q., 2014, The geochronology, geochemistry and petrogenesis of the volcanic rocks of Yeba Formation, southern Tibet (doctoral dissertation): Beijing, China University of Geosciences, p. 66.
Wei, Y.Q., Zhao, Z.D., Niu, Y.L., Zhu, D.C., Liu, D., Wang, Q., Hou, Z.Q., Mo, X.X., and Wei, J.C., 2017, Geochronology and geochemistry of the early jurassic yeba formation volcanic rocks in southern tibet: initiation of back-arc rifting and crustal accretion in the southern lhasa terrane: Lithos, v. 278–281, p. 477–490, https://doi.org/10.1016/j.lithos.2017.02.013.
Wen, D.R., 2007, The Gangdese Batholith, Southern Tibet: Ages, Geochemical Characteristics and Petrogenesis (doctoral dissertation): Department of Geosciences College of Science, National Taiwan University, P. 41–44.
Xia, B.B., Xia, B., Wang, B.D., Li, J.F., Zhang, X.G., and Wang, Y.C., 2010, Formation time of the Tangbula porphyry Mo-Cu deposit: evidence from SHRMP zircon U-Pb dating of Tangbula ore-bearing porphyries [in Chinese]: Geotectonica et Metallogenia, v. 34, p. 291–297.
Xie, F.W., Tang, J.X., Lang, X.H., and Ma, D., 2018, The different sources and petrogenesis of jurassic intrusive rocks in the southern lhasa subterrane, tibet: evidence from the trace element compositions of zircon, apatite, and titanite: Lithos, https://doi.org/10.1016/j.lithos.2018.06.024.
Xiong, Q.W., Chen, J.L., Xu, F., Huang, F., Chen, X., Zeng, Y.C., and Lei, M., 2015, LA-ICP-MS zircon U-Pb geochronology, geochemical characteristics and genetic study of Yeba Formation lavas in Demingding area, southern Tibet [in Chinese]: Geological Bulletin of China, v. 34, p. 1645–1655.
Xu, W.C., Zhang, H.F., Guo, L., and Yuan, H.L., 2010, Miocene high Sr/Y magmatism, south Tibet: Product of partial melting of subducted Indian continental crust and its tectonic implication: Lithos, v. 114, p. 293–306, https://doi.org/10.1016/j.lithos.2009.09.005.
Xu, W.C., Zhang, H.F., Luo, B.J., Guo, L., and Yang, H., 2015, Adakite-like geochemical signature produced by amphibole-dominated fractionation of arc magmas: An example from the Late Cretaceous magmatism in Gangdese belt, south Tibet: Lithos, v. 232, p. 197–210, https://doi.org/10.1016/j.lithos.2015.07.001.
Yang, Z.M., Hou, Z.Q., White, N.C., Chang, Z.S., Li, Z.Q., and Song, Y.C., 2009, Geology of the post-collisional porphyry copper-molybdenum deposit at Qulong, Tibet: Ore Geology Reviews, v. 36, p. 133–159, https://doi.org/10.1016/j.oregeorev.2009.03.003.
Zeng, Y.C., Chen, J.L., Xu, J.F., Lei, M., and Xiong, Q.W., 2017, Origin of Miocene Cu-bearing porphyries in the Zhunuo region of the southern Lhasa subterrane: Constraints from geochronology and geochemistry: Gondwana Research, v. 41, p. 51–64, https://doi.org/10.1016/j.gr.2015.06.011.
Zhang, H.F., Xu, W.C., Guo, J.Q., Zong, K.Q., Cai, H.M., and Yuan, H.L., 2007, Zircon U-Pb and Hf isotopic composition of deformed granite in the southern margin of the Gangdese belt, Tibet: Evidence for early Jurassic subduction of Neo-Tethyan oceanic slab [in Chinese]: Yanshi Xuebao, v. 23, p. 1347–1353.
Zhang, L.L., Liu, C.Z., Wu, F.Y., Ji, W.Q., and Wang, J.G., 2014, Zedong terrane revisited: An intra-oceanic arc within Neo-Tethys or a part of the Asian active continental margin?: Journal of Asian Earth Sciences, v. 80, p. 34–55, https://doi.org/10.1016/j.jseaes.2013.10.029.
Zhang, L.L., Liu, C.Z., Wu, F.Y., Zhang, C., Ji, W.Q., and Wang, J.G., 2016, Sr–Nd–Hf isotopes of the intrusive rocks in the Cretaceous Xigaze ophiolite, southern Tibet: Constraints on its

formation setting: Lithos, v. 258–259, p. 133–148, https://doi.org/10.1016/j.lithos.2016.04.026.
Zhang, Z.M., Zhao, G.C., Santosh, M., Wang, J.L., Dong, X., and Shen, K., 2010, Late Cretaceous charnockite with adakitic affinities from the Gangdese batholith, southeastern Tibet: Evidence for Neo-Tethyan mid-ocean ridge subduction?: Gondwana Research, v. 17, p. 615–631, https://doi.org/10.1016/j.gr.2009.10.007.
Zhao, J.X., Qin, K.Z., Li, G.M., Li, J.X., Xiao, B., and Chen, L., 2012, Geochemistry and petrogenesis of granitoids at sharang eocene porphyry mo deposit in the main-stage of india-asia continental collision, northern gangdese, tibet: Resource Geology, v. 62, p. 84–98, https://doi.org/10.1111/j.1751-3928.2011.00181.x.
Zheng, Y.C., Hou, Z.Q., Gong, Y.L., Liang, W., Sun, Q.Z., Zhang, S., Fu, Q., Huang, K.X., Li, Q.Y., and Li, W., 2014, Petrogenesis of Cretaceous adakite-like intrusions of the Gangdese Plutonic Belt, southern Tibet: Implications for mid-ocean ridge subduction and crustal growth: Lithos, v. 190–191, p. 240–263, https://doi.org/10.1016/j.lithos.2013.12.013.
Zheng, Y.C., Hou, Z.Q., Li, Q.Y., Liang, W., Fu, Q., Li, W., and Huang, K.X., 2012, Origin of Late Oligocene adakitic intrusives in the southeastern Lhasa terrane: evidence from in situ zircon U–Pb dating, Hf–O isotopes, and whole-rock geochemistry: Lithos, v. 148, p. 296–311, https://doi.org/10.1016/j.lithos.2012.05.026.
Zhou, L.M., Wang, R., Hou, Z.Q., Li, C., Zhao, H., Li, X.W., and Qu, W.J., 2018, Hot Paleocene-Eocene Gangdese arc: Growth of continental crust in southern Tibet: Gondwana Research, v. 62, p. 178–197, https://doi.org/10.1016/j.gr.2017.12.011.
Zhu, D.C., Pan, G.T., Chung, S.L., Liao, Z.L., Wang, L.Q., and Li, G.M., 2008, SHRIMP Zircon Age and Geochemical Constraints on the Origin of Lower Jurassic Volcanic Rocks from the Yeba Formation, Southern Gangdese, South Tibet: International Geology Review, v. 50, p. 442–471, https://doi.org/10.2747/0020-6814.50.5.442.
Zhu, D.C., Zhao, Z.D., Niu, Y.L., Mo, X.X., Chung, S.L., Hou, Z.Q., Wang, L.Q., and Wu, F.Y., 2011, The Lhasa Terrane: Record of a microcontinent and its histories of drift and growth: Earth and Planetary Science Letters, v. 301, p. 241–255, https://doi.org/10.1016/j.epsl.2010.11.005.
Zhu, D.C., Zhao, Z.D., Pan, G.T., Lee, H.Y., Kang, Z.Q., Liao, Z.L., Wang, L.Q., Li, G.M., Dong, G.C., and Liu, B., 2009, Early cretaceous subduction-related adakite-like rocks of the Gangdese Belt, southern Tibet: Products of slab melting and subsequent melt-peridotite interaction?: Journal of Asian Earth Sciences, v. 34, p. 298–309, https://doi.org/10.1016/j.jseaes.2008.05.003.

εNd(t=15 Ma)

εHf(t=15 Ma)

(A)

Jurassic sample with the highest value of $\varepsilon Nd_{(t)}$ per 0.5 longitude

Average $\varepsilon Nd_{(t)}$ of Jurassic samples per 0.5 longitude

(B)

Cretaceous sample with the highest value of $\varepsilon Nd_{(t)}$ per 0.5 longitude

Average $\varepsilon Nd_{(t)}$ of Cretaceous samples per 0.5 longitude

(C)

Paleocene-Eocene sample with the highest value of $\varepsilon Nd_{(t)}$ per 0.5 longitude

Average $\varepsilon Nd_{(t)}$ of Paleocene samples per 0.5 longitude

(D)

Miocene sample with the highest value of $\varepsilon Nd_{(t)}$ per 0.5 longitude

Average $\varepsilon Nd_{(t)}$ of Miocene samples per 0.5 longitude

(E)

Jurassic sample with the highest value of $\varepsilon Hf_{t)}$ per 0.5 longitude

Average $\varepsilon Hf_{t)}$ of Jurassic samples per 0.5 longitude

(F)

Cretaceous sample with the highest value of $\varepsilon Hf_{t)}$ per 0.5 longitude

Average $\varepsilon Hf_{t)}$ of Cretaceous samples per 0.5 longitude

(G)

Paleocene-Eocene sample with the highest value of $\varepsilon Hf_{t)}$ per 0.5 longitude

Average $\varepsilon Hf_{t)}$ of Paleocene samples per 0.5 longitude

(H)

Miocene sample with the highest value of $\varepsilon Hf_{t)}$ per 0.5 longitude

Average $\varepsilon Hf_{t)}$ of Miocene samples per 0.5 longitude

longitude (°E)

longitude (°E)

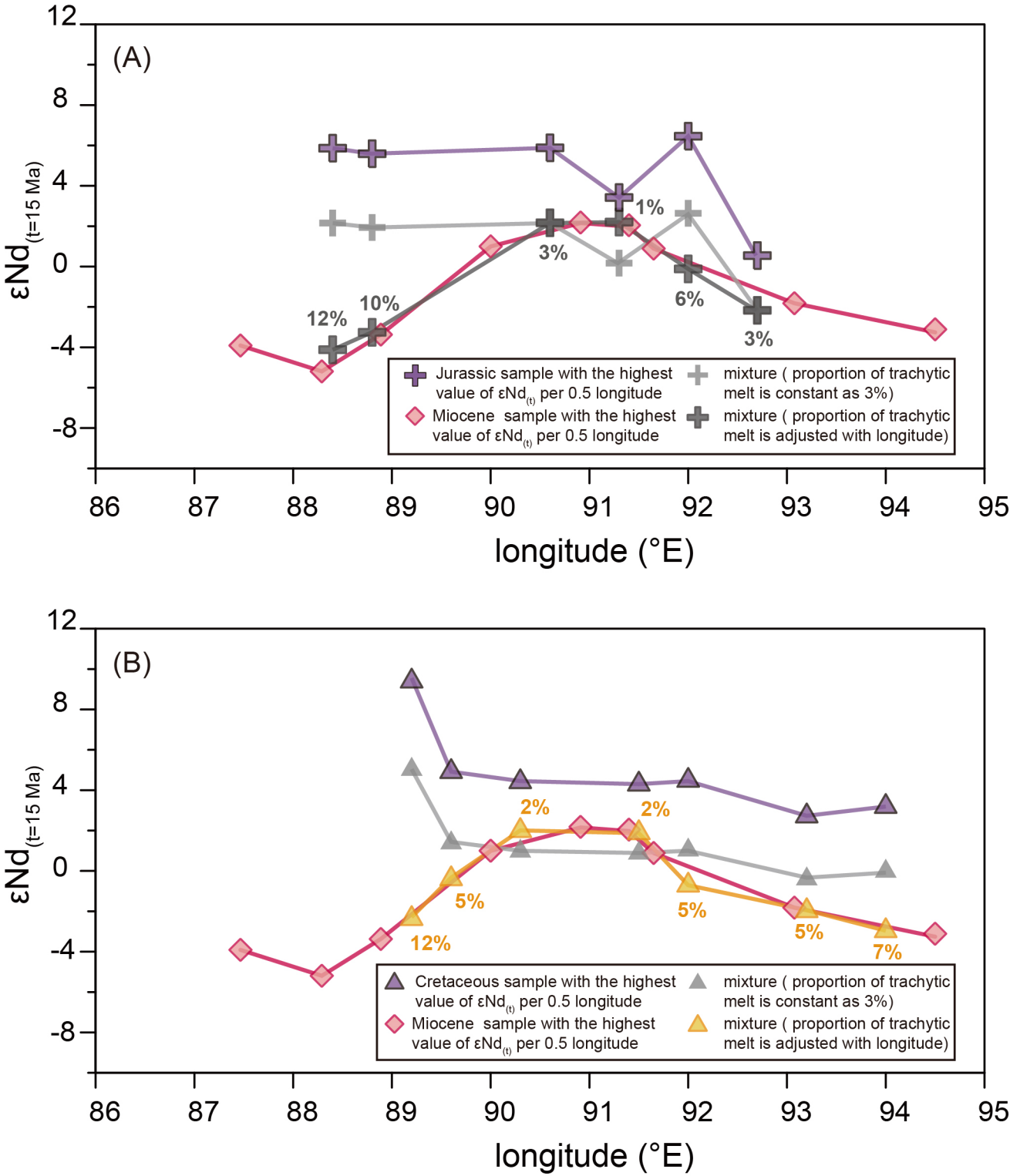
(A)
εNd(t=15 Ma)
longitude (°E)
1%
3%
6%
3%
12%
10%
Jurassic sample with the highest value of εNd(t) per 0.5 longitude
Miocene sample with the highest value of εNd(t) per 0.5 longitude
mixture (proportion of trachytic melt is constant as 3%)
mixture (proportion of trachytic melt is adjusted with longitude)
(B)
εNd(t=15 Ma)
longitude (°E)
2%
2%
5%
5%
5%
12%
7%
Cretaceous sample with the highest value of εNd(t) per 0.5 longitude
Miocene sample with the highest value of εNd(t) per 0.5 longitude
mixture (proportion of trachytic melt is constant as 3%)
mixture (proportion of trachytic melt is adjusted with longitude)